Model predictive control applied to hybridised modular fuel cell systems

Noé Rivier, Pauline Kergus, Jérémi Regnier, Amine Jaafar, Christophe Turpin, Chouaib Afri, Paul Boucharel, Jérôme Lachaize, Malik Tognan

Model predictive control applied to hybridised modular fuel cell systems

Noé Rivier[1], Pauline Kergus[1], Jérémi Regnier[1], Amine Jaafar[1], Christophe Turpin[1], Chouaib Afri [2],Paul Boucharel[2], Jérôme Lachaize[2], Malik Tognan[3]

Abstract

This paper proposes a predictive control strategy to minimize the hydrogen consumption of a modular fuel cell system hybridized with a battery. This approach is compared with a reference solution obtained using optimal control. By increasing the prediction horizon, performances tends to the reference ones, minimizing the consumption and aging of the modules while maintaining a solution that can be implemented online. It is shown that the gains in energy consumption and module aging are achieved at the expense of battery aging in both cases.

1 Introduction

Hydrogen is recognized as a potential solution for decarbonizing the heavy mobility sector. For this technology to become widespread, it is necessary to reduce the hydrogen consumption of the hybrid fuel cell hybrid electric vehicle (FCHEV) and increase their lifespan. This requires enhancement of PEMFC-LT (Proton Exchange Membrane Fuel Cell Low Temperature) technology and the implementation of more efficient energy distribution strategies. Among the various control techniques, model predictive control (MPC) has attracted attention for FCHEV as it can handle constrained systems efficiently[1]. For fuel cell hybridized with a battery [2, 3, 4], MPC allows to anticipate the evolution of the state of charge of the battery and reduce the consumption over a driving cycle. In this regard, the contribution of this

*This work is part of the ECH2 project, financed by the French Government as part of the France 2030 plan operated by ADEME. The consortium is composed of: ALSTOM Hydrogène SAS, Siemens Digital Industries Software, IFP Energies Nouvelles, Vitesco Techonologies, Institut de Mathématiques de Toulouse and LAPLACE.

*Corresponding autor : rivier@laplace.univ-tlse.fr

*1 LAPLACE, Université de Toulouse, CNRS, INPT, UPS, Toulouse, France.

*2 Vitesco Technologies, Toulouse, France.

*3 H2 Pulse, Toulouse, France

paper resides in adressing the impact of predictive control on battery and fuel cell ageing as well as hydrogen consumption.

In this paper, a MPC strategy is proposed to minimize hydrogen consumption for an hybridized modular fuel cell system for heavy-duty vehicles. The impact on fuel cell and battery aging is analyzed, as well as the influence of the choice of prediction horizon. To that extent, a reference solution is obtained by solving the corresponding optimal control problem, offline and a posteriori, with perfect knowledge of the full driving cycle.

This paper is organized as follows. Section 2 details the models describing the considered system. Section 3.1 presents the reference dispatch strategy, which solves the optimal control problem offline and a posterioti. Section 3.2 describes the predictive control strategy and its implementation. Section 4 compares both strategies for different forecast horizons, in terms of hydrogen consumption and aging.

2 Considered system

The system under consideration consists of 3 fuel cell (FC) modules hybridized with a battery, it is designed for designed for heavy goods vehicles up to 40 tonnes. It is described by a FC operation model, a FC aging model, a battery operation model and a battery aging model. The entire system is controlled by the power strategy, which is the focus of this paper. Two optimisation based strategies are presented and compared. The details of the sub-models are given in the following subsections.

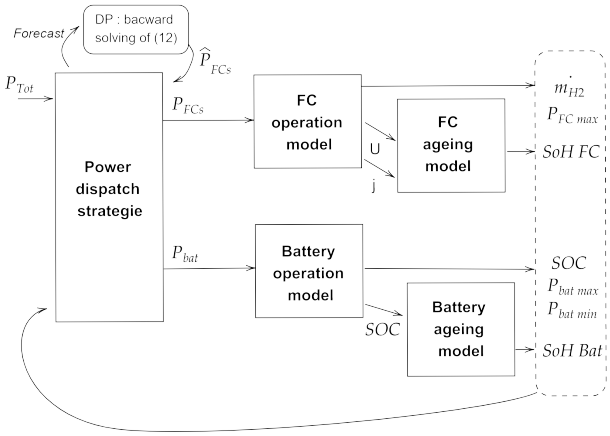

Figure 1: Architecture of the considered model: the required power (P_{tot}) is dispatched between the Fuel cell system (FCs) and the battery. From this distribution, the sub-models update the state variables and the state of health.

2.1 FC operation model

The model consists in a mapping of the performance of a FC stack given by a tabulation. For a given current density j and State of Health (SoH), defined by the FC aging model, a table gives the net power output of the module.

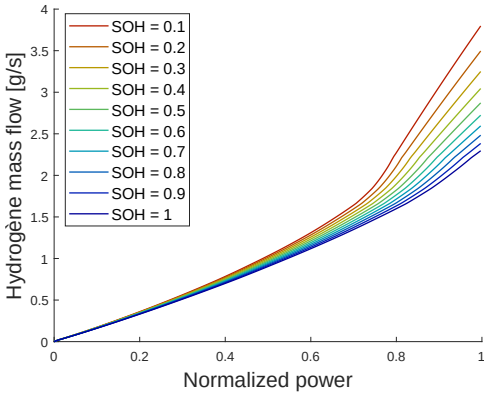

Figure 2: Module H2 consumption curve as a function of power for different SoH

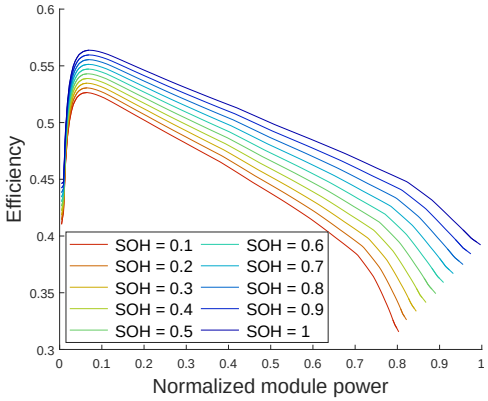

Figure 3: Module's efficiency curve as a function of power for different SoH

Similarly, the hydrogen consumption of each module $\dot{m}_{iH_2}$ is tabulated (Figure 2). For a power demand, the module consumption increases as the SoH of the module deteriorates. The energy efficiency of a module is defined on the basis of its consumption $\dot{m}_{iH_2}$ [g/s], the lower heating value of the dihydrogen LHV_{H_2} [J/g] and its power P_i.

$$\eta_i = \frac{P_i}{\dot{m}_{i\ H_2} * LHV_{H_2}} \tag{1}$$

To account for the compressor's inertia, the model limits the modules power variations in the following way:

$$P_i^{max}(t+1) = P_i(\dot{m}_{air}^{max}(t+1)), \tag{2}$$

where the maximum air flow of the compressor $\dot{m}_{air}^{max}$ is given by:

$$\dot{m}_{air}^{max}(t+1) = \dot{m}_{air}(t) + \Delta\dot{m}_{air}^{max}, \tag{3}$$

where $\Delta\dot{m}_{air}^{max} = 0.0707\ [kg.s^{-2}]$.

2.2 FC aging model

In this paper, the FC aging model is based on the superposition principle as in [5] [6] [7]. It identifies specific degrading operating regimes and the corresponding voltage drop of the fuel cells. Four degrading regimes are considered:

- Start degradation δ^{ss} [V]: if the i module switches from off to on $\delta_i^{ss} = \delta_{ref}^{ss}$, otherwise $\delta_i^{ss} = 0$.
- Open Circuit Voltage (OCV) δ^{OCV} [V]: when a module's voltage approaches its OCV, i.e. when $U > U^*$,

  $$\delta^{OCV} = k_{OCV}(U - U^*)^{n_{OCV}}$$

  with $U^* = 0.802[V]$. When $U <= U^*$,

  $$\delta^{OCV} = 0$$

- Operational degradation δ^j [V]:the degradation are proportionals to the current density within the FC cells:

  $$\delta^j = k_j j$$

  with j the current density in $[A.cm^{-2}]$.
- Power transition δ^{pt} [V]: only increases in power are counted, as the model assumes that a drop in the power supplied by a module does not cause any damage.

  $$\delta^{pt} = k_{pt} \frac{j}{J_{lim}} \frac{\Delta j}{J_{lim} - \Delta j}^{n_{pt}}$$

  Where Δj is the variation in current density over one second, $J_{lim} = 2.35\ [A.cm^{-2}]$.

Table 1: aging model coefficients

Coefficient	δ_{ref}^{ss}	k_{OCV}	n_{OCV}	k_j	k_{pt}	n_{tp}
Value	2e-6	7.09e-7	2	2.49e-9	7.81e-6	2

The above coefficients (Table 1) have been adjusted based on a FC load derived from a Hyundai Nexo over a WLTC homologation cycle and an expected life of 10,000 hours at this load. This model and its parameters have not yet been experimentally validated.

Based on these 4 degradation regimes, the model calculates the instantaneous degradation $\delta_i^{tot}(t)$ of each module:

$$\delta_i^{tot}(t) = \delta_i^{ss}(t) + \delta_i^{OCV}(t) + \delta_i^{j}(t) + \delta_i^{tp}(t) \tag{4}$$

then the (SoH) variation of the modules $d_{SoH\ i}(t)$.

$$d_{SoH\ i}(t) = \frac{\delta_i^{tot}(t)}{\Delta V_{margin}} \tag{5}$$

Where ΔV_{margin} represents the maximum acceptable voltage drop to consider that a cell is still in working order and $\delta_i^{tot}(t)$ the total instantaneous degradation of the i module at time t. The SoH of modules is updated as follow:

$$SoH_i(t_k + 1) = SoH_i(t_k) + \int_{t_k}^{t_k+1} d_{SoH\ i}(t)dt \tag{6}$$

When a FC module is new, its (SoH) is equal to 1. When the SoH reaches 0, the module is considered to have reached the end of its life. Using the curve bundle in Figure 3, the aging of modules is reflected in their performance during a simulation.

2.3 Battery operation model

The battery operation model used is an internal resistance model, its parameters have been extracted from an internal resistance model of the Simcenter AMESim software, validated on experimental data [8]. The battery power and its voltage are given by:

$$\begin{cases} P_{bat} = U_b * I_b \\ U_b = U_{bat\ ocv} - I_b * R_b(SoC, P_{bat}) \end{cases} \tag{7}$$

Where $U_{bat\ ocv}$ is the open circuit voltage of the battery, I_b is the current flowing through the battery and $R_b(Soc, P_{bat})$ is its internal resistance varying with the state of charge (SoC) of the battery and the sign of P_{bat}. In this work it is obtained from a tabulation. For a given battery power P_{bat} and charge level SoC, I_b is calculated as follows:

$$I_b = \frac{U_{bat\ ocv} - \sqrt{U_{bat\ ocv}^2 - 4R_b(Soc, P_{bat})P_{bat}}}{2R_b(Soc, P_{bat})} \tag{8}$$

From I_b the model estimates the variation in the battery's state of charge (d_{SoC}) using the following formula:

$$d_{SoC} = \frac{-I_b}{3600 * Q_{bat}} \tag{9}$$

Where Q_{bat} represents the battery storage capacity. The SoC is updated as follow:

$$SoC(t_k + 1) = SoC(t_k) + \int_{t_k}^{t_k+1} d_{SoC}(t)dt \tag{10}$$

2.4 Battery aging model

The battery aging model used in this word is based on the work of [9] [10] . Due to limitations in space, it is not possible to develop this model in this paper. For a given battery power, SoC and capacity, it returns the updated battery capacity and the corresponding capacity loss.

2.5 Simulated scenarios

In this paper, the reference strategy and the MPC are compared over a Lyon-Milan driving cycle (Figure 4).

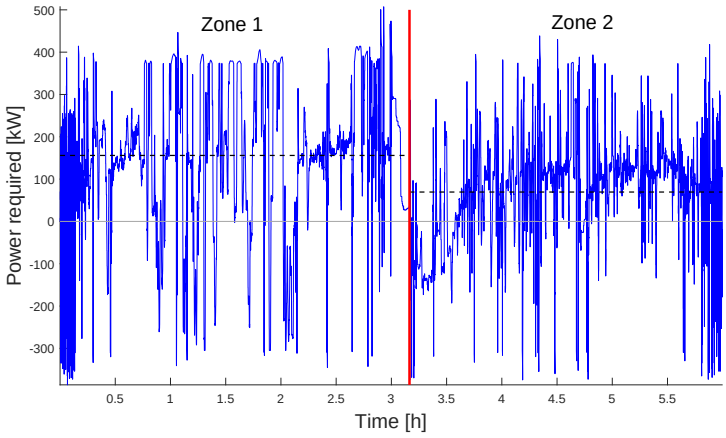

Figure 4: Full driving cycle power profile. Two distinct zones can be identified. In the first half (zone 1), the vehicle ascends to cross the Alps, requiring a high average power (shown in dashed black). In the second half (zone 2), the vehicle descends, requiring less average power.

It is assumed that, over the 6-hour driving cycle, fuel cells do not age enough to cause significant over-consumption. For this reason, a constant SoH is assumed when solving the optimal control and MPC optimisation problems. Aging is then accounted for when simulating the resulting power dispatch strategies.

3 Methodology

3.1 Optimal control

The considered optimal control problem is as follows:

$$\begin{aligned} \min_{P_{FCs}} \quad & \sum_{t=t_0}^{t_{end}} \dot{m}_{H_2\ FCs}(t) \\ \text{s.t.} \quad & P_{FCs} + P_{bat} = P_{tot} \\ & 0 \leq P_{FCs} \leq P_{FCs}^{max} \\ & P_{bat}^{min} \leq P_{bat} \leq P_{bat}^{max} \\ & SoC(t_{end}) = SoC_{target} \end{aligned} \tag{11}$$

where P_{tot} is the total power to be supplied by the system, P_{FCs} the power supplied by the FC system and P_{bat} the power supplied by the battery. $\dot{m}_{H_2\ FCs}(t)$ is the hydrogen consumption of the multi-modular system for a given time step.

It minimizes consumption over the entire driving cycle. It is solved backward by dynamic programming (DP) using [11]. The solution is guaranteed to be optimal for a given model and discretisation step. As this method requires knowledge of the entire driving cycle and is computationally expensive, it is not suitable for online applications and should be regarded as a reference solution to tend to. In this paper, the optimal control solution is used as a reference to evaluate the MPC strategy.

3.2 Model predictive control

In this section, the power dispatch strategy consists of a model predictive controller. It takes forecast of the power demand as an input to determine the dispatch at each time. The optimisation problem is similar to (11) but covers a shorter and moving prediction horizon rather than the complete driving cycle. This renders the method suitable for online implementation.

The MPC solves the following optimisation problem for every time step of the driving cycle:

$$\begin{aligned} \min_{P_{FCs}} \quad & \sum_{t=t_k}^{t_k+H} \dot{m}_{H_2\ FCs}(t) \\ \text{s.t.} \quad & P_{FCs} + P_{bat} = P_{tot} \\ & 0 \leq P_{FCs} \leq P_{FCs}^{max} \\ & P_{bat}^{min} \leq P_{bat} \leq P_{bat}^{max} \\ & SoC(t_k + H) = SoC_{target} \end{aligned} \tag{12}$$

where P_{tot} is the total power to be supplied by the system, P_{FCs} the power supplied by the FC system and P_{bat} the power supplied by the battery.

$\dot{m}_{H_2\ FCs}(t)$ is the hydrogen consumption of the multi-modular system for a given time step.

As for optimal control, problem (12) is solved through DP using [11]:

- If the problem is feasible, the DP algorithm returns a vector of optimal commands for the next H seconds. The first instant of the command is applied as the power setpoint for the multi-modular system.
- Sometimes the SoC constraint from (12) is infeasible. This occurs, for instance, when the state of charge (SoC) at a given time t is less than the target SoC and the average predicted power is greater than the maximum power that can be supplied by the fuel cell stack P_{FCs}^{max}. In this case, the battery is forced to have an energy deficit over the prediction horizon in order to meet the power demand. Consequently, the SoC is forced to fall, and the constraint $SoC(t+H) = SoC_{target}$ cannot be met.

In the event that (12) is infeasible, the battery SoC is compelled to decline. To mitigate this, the modules operate at maximum power, limiting SoC drop. Increasing the value of the forecast horizon reduces the number of instances where the optimisation problem becomes infeasible.

4 Results

In this section, the two methods presented in the previous section are applied on the driving cycle visible on Figure 4. It should be recalled that optimal control is considered as a reference to evaluate the performances of the MPC, and will be referred to as the reference solution in this section.

The power distribution achieved by predictive control with a prediction horizon $H = 350$ and the reference solution are shown on Figure 5a . While MPC covers a much wider range of power, it is more responsive to variations in the driving cycle. The reference power distribution reflects particularly well the two stages of the driving cycle, with a first zone of high power and a second of medium power.

Figure 6 shows the frequency at which the modules are used for different power ranges over the driving cycle. The results are indicated for several predictive control horizons along with the reference solution. As the prediction horizon increases, the modules spend less time operating at very low and very high power levels. This is reflected in the narrowing of the histogram of MPC around low to medium power levels, which corresponds to the area of maximum module efficiency. The power distribution appears to tend towards that of the reference solution, which is a logical consequence of the similarity of the respective optimisation problems.

It results in a diminution in both consumption and modules aging, which are represented on Figure 7. A shift from a five-second prediction horizon

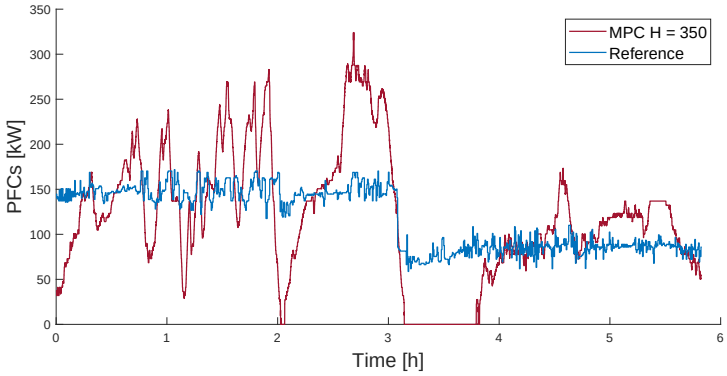

(a) Modules power over the driving cycle for both strategies. The reference power distribution is smoothed around two values, each corresponding to a zone in the driving cycle (see Figure 4)

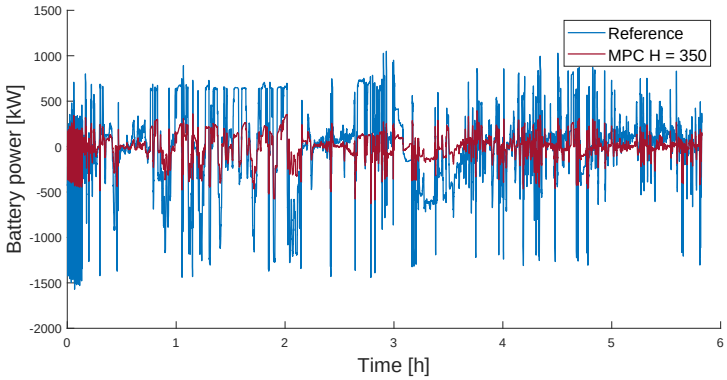

(b) Battery power over the driving cycle for both strategies. In the reference case, the battery absorbs all the variations in power required by the driving cycle. Predictive control allows less variations of battery power as the driving cycle variations are absorded by the modules.

Figure 5: Power distribution for both strategies

to 350 seconds allows for a notable reduction in overconsumption, from approximately 13% to 2%. As the prediction horizon is extended beyond 350 seconds, the points become more compact. Doubling the prediction horizon from 300 seconds to 600 seconds results in consumption gains of less than 1%.

As the prediction horizon increases, power fluctuations are reduced, leading to a significant decrease in power transients and a reduction in the time the modules spent operating at low power. This limits the open circuit voltage degradation. However, as the modules operate more frequently at medium power levels, the operational degradation slightly increases. We can also notice a reduction of module stops, resulting in a decrease of start-stop degradation. This is visible on Figure 8. It should be noted that if the

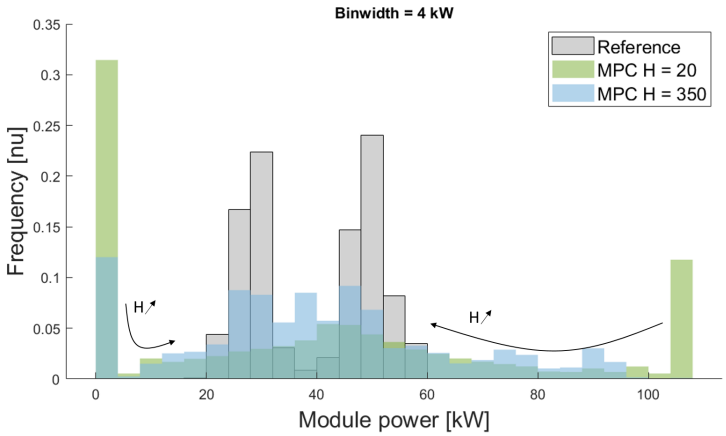

Figure 6: Histogram of the power supplied by the modules over the driving cycle for each strategy. As the prediction horizon increases, the histogram of MPC narrows around low to medium power levels, corresponding to the area of maximum module efficiency.

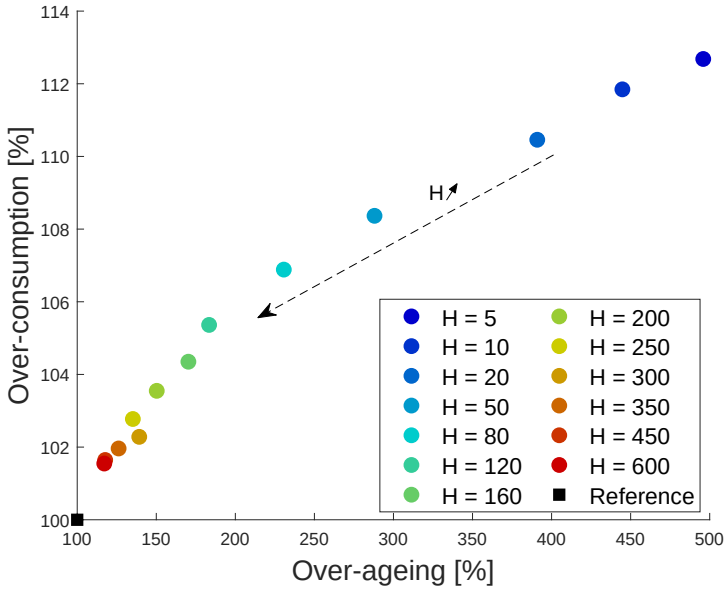

Figure 7: Hydrogen consumption and voltage drops induced by each distribution strategy are expressed relatively to the reference solution.

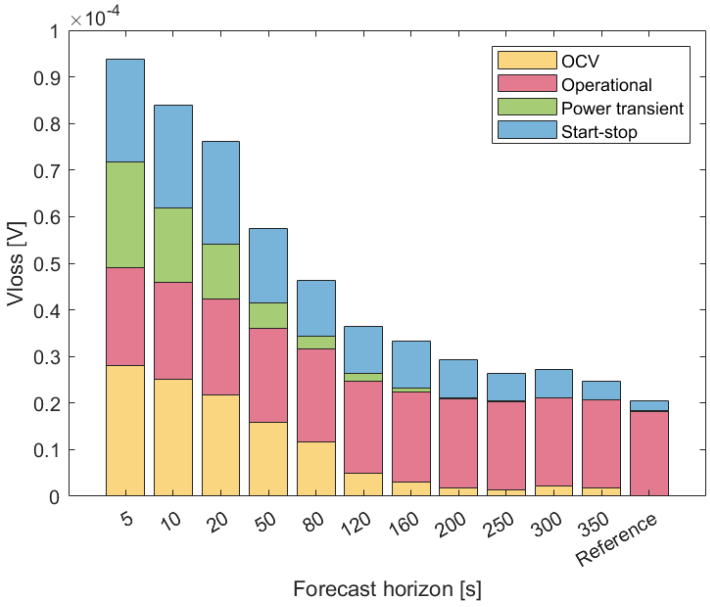

Figure 8: Impact of the forecast horizon on the FC degradation. $V_{loss} = SoH(t_{end}) * \Delta V_{margin}$ represents the voltage drop for a fuel cell over the driving cycle.

MPC reduces both the consumption and the FC ageing, only the hydrogen consumption is part of the cost function (12). In addition to reducing power transition, OCV and start-stop degradation, the power range of high efficiency and the power range of low operationnal degradation are coincident.

As the prediction horizon increases, the MPC has a longer time horizon to ensure that the SoC remains above 50%. This allows for longer charge and discharge of the battery (Figures 5b and 9), leading to a reduction in battery capacity (Table 2). For the reference solution, module aging and consumption are much lower than with predictive control, but at the cost of a very sharp deterioration in battery capacity, due to the over solicitation of the battery (as seen in Figures 5b and 9).

Table 2: Capacity loss (Q_{loss}) of a battery cell for different strategies

Strategies	**DP**	**MPC H = 350**	**MPC H = 5**
Q_{loss} [A.h]	6.600e-2	1.906e-2	1.238e-2
$\frac{Q_{loss}}{Q_{loss\ Reference}}$	1	0.288	0.1875

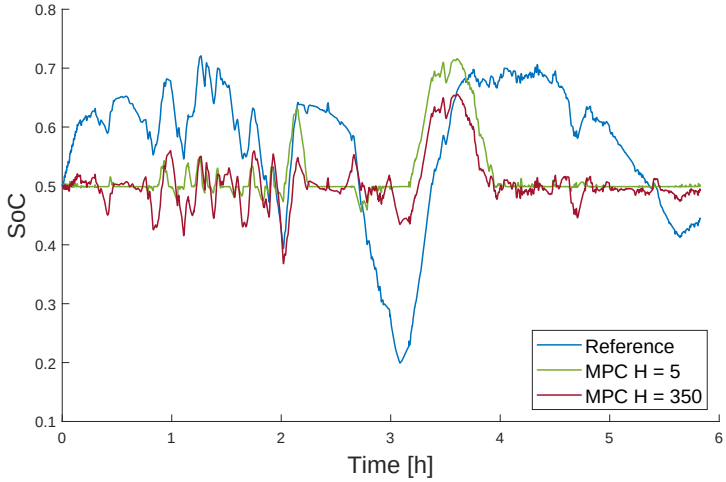

Figure 9: Evolution of the battery SoC over the driving cycle for each strategies. In order to minimize consumption over the driving cycle, the dynamic programming solution uses almost the full amplitude allowed by the battery [0.2-0.8]. The SoC induced by predictive control remains fairly stable around 0.5.

5 Conclusions and outlooks

In this paper, a MPC strategy that minimizes hydrogen consumption has been implemented to dispatch power in a hybridized modular fuel cell system for heavy-duty transportation. The results are evaluated by comparison with a reference case which is the solution of the corresponding optimal control problem, solved offline and a posteriori for the whole driving cycle.

The longer the prediction horizon, the more information the MPC has to manage power distribution. This allows to limit high power operation and shut down modules less frequently. The power demanded from the modules is smoother, reducing the degradation associated with OCV, high power, power transients and start-stops. Both consumption and module aging are reduced by extending the prediction horizon. However, the battery is more stressed, increasing its corresponding degradation.

In this work the cost function only minimises the hydrogen consumption, to limit the burden on the battery it would be interesting to include the battery aging in the objective function. Moreover, the prediction provided to the MPC is assumed to be accurate. Future work will study the impact of an error in the prediction on the performance of the MPC.

Acknowledgment

This work is part of the ECH2 project, funded by the French Government as part of the France 2030 plan operated by ADEME. The consortium is composed of: ALSTOM Hydrogène SAS, Siemens Digital Industries Software, IFP Energies Nouvelles, Vitesco Techonologies, Institut de Mathématiques de Toulouse and LAPLACE.

References

[1] S. Quan, Y.-X. Wang, X. Xiao, H. He, and F. Sun, "Real-time energy management for fuel cell electric vehicle using speed prediction-based model predictive control considering performance degradation," *Applied Energy*, vol. 304, p. 117 845, Dec. 15, 2021, ISSN: 0306-2619. DOI: 10.1016/j.apenergy.2021.117845.

[2] A. Ferrara, M. Okoli, S. Jakubek, and C. Hametner, "Energy Management of Heavy-Duty Fuel Cell Electric Vehicles: Model Predictive Control for Fuel Consumption and Lifetime Optimization," *IFAC-PapersOnLine*, 21st IFAC World Congress, vol. 53, no. 2, pp. 14 205–14 210, Jan. 1, 2020, ISSN: 2405-8963. DOI: 10.1016/j.ifacol.2020.12.1053.

[3] A. Arce, A. J. del Real, and C. Bordons, "MPC for battery/fuel cell hybrid vehicles including fuel cell dynamics and battery performance improvement," *Journal of Process Control*, Special Section on Hybrid Systems: Modeling, Simulation and Optimization, vol. 19, no. 8, pp. 1289–1304, Sep. 1, 2009, ISSN: 0959-1524. DOI: 10.1016/j.jprocont.2009.03.004.

[4] D. Shen, C.-C. Lim, and P. Shi, "Robust fuzzy model predictive control for energy management systems in fuel cell vehicles," *Control Engineering Practice*, vol. 98, p. 104 364, May 1, 2020, ISSN: 0967-0661. DOI: 10.1016/j.conengprac.2020.104364.

[5] J. M. Desantes, R. Novella, B. Pla, and M. Lopez-Juarez, "A modeling framework for predicting the effect of the operating conditions and component sizing on fuel cell degradation and performance for automotive applications," *Applied Energy*, vol. 317, p. 119 137, Jul. 1, 2022, ISSN: 0306-2619. DOI: 10.1016/j.apenergy.2022.119137.

[6] Z. Hu *et al.*, "Multi-objective energy management optimization and parameter sizing for proton exchange membrane hybrid fuel cell vehicles," *Energy Conversion and Management*, vol. 129, pp. 108–121, Dec. 1, 2016, ISSN: 0196-8904. DOI: 10.1016/j.enconman.2016.09.082.

[7] A. Pessot *et al.*, "Development of an aging estimation tool for a pem fuel cell submitted to a mission profile," *Fuel Cells*, vol. 20, no. 3, pp. 253–262, 2020.

[8] E. Prada, J. Bernard, R. Mingant, and V. Sauvant-Moynot, "Li-ion thermal issues and modeling in nominal and extreme operating conditions for HEV / PHEV's,"

[9] I. Bloom *et al.*, "An accelerated calendar and cycle life study of Li-ion cells," *Journal of Power Sources*, vol. 101, no. 2, pp. 238–247, Oct. 15, 2001, ISSN: 0378-7753. DOI: 10.1016/S0378-7753(01)00783-2.

[10] C. Guenther, B. Schott, W. Hennings, P. Waldowski, and M. A. Danzer, "Model-based investigation of electric vehicle battery aging by means of vehicle-to-grid scenario simulations," *Journal of Power Sources*, vol. 239, pp. 604–610, Oct. 1, 2013, ISSN: 0378-7753. DOI: 10.1016/j.jpowsour.2013.02.041.

[11] O. Sundstrom and L. Guzzella, "A generic dynamic programming Matlab function," in *2009 IEEE International Conference on Control Applications*, St. Petersburg, Russia: IEEE, Jul. 2009, pp. 1625–1630, ISBN: 978-1-4244-4601-8. DOI: 10.1109/CCA.2009.5281131.